Potential role of pre-existing blood vessels for vascularization and mineralization of osteochondral grafts

An intravital microscopic study in mice

Dominique A Rothenfluh[1, 2], Thomas J Demhartner[1], Christian R Fraitzl[1], Marco G Cecchini[2], Reinhold Ganz[1] and Michael Leunig[1]

Departments of [1]Orthopedic Surgery, University of Berne, Inselspital, CH-3010 Berne, [2]Clinical Research, University of Berne, CH-3010 Berne, Switzerland
Correspondence DR: drothenfluh@swissonline.ch
Submitted 02-03-19. Accepted 03-05-24

Background **The aim of this study was to develop an experimental model that allows to elude the potential role of the preexisting graft microvasculature for vascularization and mineralization of osteochondral grafts.**

Animals and methods **For that purpose, the II-IV metatarsals of fetal DDY-mice known to be nonvascularized at day 16 of gestation (M16) but vascularized at day 18 (M18) were freshly transplanted into dorsal skin fold chambers of adult DDY mice. Using intravital microscopy angiogenesis, leukocyte-endothelium interaction and mineralization were assessed for 12 days.**

Results **Angiogenesis occurred at 32 hours in M18, but not before 57 hours in M16 ($p = 0.002$), with perfusion of these vessels at 42 hours ($p = 0.005$) and 65 hours ($p = 0.1$), respectively. Vessels reached a density three times as high as that of the recipient site at day 6, remaining constant until day 12 in M18, whereas in M16 vascular density increased from day 6 and reached that of M18 at day 12 ($p = 0.04$). Leukocyte-endothelium interaction showed sticker counts elevated by a factor of 4-5 in M18 as compared to M16. Mineralization of osteochondral grafts did not differ between M16 and M18, which significantly increased in both groups throughout the observation period.**

Interpretation **We propose the faster kinetics in the angiogenic response to M18 and the elevated counts of sticking leukocytes to rest on the potential of establishing end-to-end anastomoses (inosculation) of the vascularized graft with recipient vessels.**

Incorporation of bone grafts involves a cascade of biological events similar to those observed during wound healing (Glowacki 1998). As evidenced by intravital microscopy, angiogenesis precedes osteogenesis (Albrektsson and Albrektsson 1978, Albrektsson 1980), representing an important event for the viability and incorporation of bone (Burchardt 1987). Experimental studies have shown that rapidly vascularized bone grafts retain their viability and demonstrate improved incorporation (Puckett et al. 1979). To date, the potential contribution of donor-derived microvessels for the viability and incorporation of bone grafts has not been addressed. For this purpose, we have established a mouse model which allows the transplantation of nonvascularized and vascularized osteochondral grafts. In this model, metatarsals of defined developmental stages implanted in dorsal skin fold chambers are subjected to intravital microscopy in order to study the potential contribution of donor-derived blood vessels for the revascularization and mineralization of bone grafts. The hypothesis underlying this study was that donor-derived microvessels contribute to the vascularization and mineralization of fresh osteochondral grafts.

Animals and methods

Preparation of dorsal skin fold chamber

We used adult, male DDY mice (weight 25–30 g). Under general anesthesia (ketamine/xylazine 7.5 mg/2.5 mg per 100 g b.w. i.m) the depilated dorsal skin fold was raised and two symmetrical titanium frames were mounted so as to sandwich the extended double layer of the skin. One layer of the skin fold was removed in a circular area of approximately 15 mm in diameter. The remaining layer, consisting of epidermis, dermis, subcutaneous tissue and striated skin muscle, was dissected microsurgically and freed from connective and adipose tissue to ensure good visualization of microvessels within the striated skin muscle and subcutaneous tissue. Thereafter, the chamber preparation was covered by a removable glass coverslip being incorporated into one of the frames (Leunig et al. 1996).

After a recovery period of 48 hours, chambers meeting our criteria for intact microcirculation were used for implantation. These criteria included (i) the absence of pus or bleeding, (ii) absence of surgical trauma or trauma-induced angiogenesis, (iii) absence of congestion in the post-capillary and venous vessels (venular blood flow velocity > 0.3 mm/sec), (iv) no kinking or dilation of post-capillary and venous vessels, and (v) an arteriolar/venular diameter ratio of 1/3 to 1/4.

Preparation of metatarsals

We used the three middle metatarsals (II–IV) of each paw for transplantation, as they show a synchronized process of mineralization during mouse development (Wirtschafter 1960). After decapitation, the mice were kept in 70% ethanol for 5 min to reduce skin contamination by pathogens. Metatarsals of 16 (M16) and 18 (M18) day-old fetal DDY mice were blunt dissected in 5 mL Dulbecco's modified Eagle's medium (DMEM; Seromed, Bichron, Berlin, Germany) at room temperature (22 °C). To remove the periosteum completely, metatarsals were incubated with 0.1% collagenase for 5 min and soft tissues were mechanically stripped by rolling the bone explants on a plastic surface under microscopic control. Thereafter, the metatarsals were transferred to a second dish containing fresh DMEM at 4 °C and implanted within the first hours after retrieval. Only metatarsals without signs of cartilage or bone damage were used for implantation (success rate 85%). Nonvascularized M16 and vascularized M18 metatarsals were isogenically transplanted (DDY to DDY). The metatarsals of each group were implanted into DDY mice fitted with the dorsal skin fold chamber as follows: 5 mice with M16 revealed 3, 4, 2, 3 and 3 metatarsals accessible to intravital microscopy in each chamber; 4 mice with M18 revealed 4, 3, 4 and 4 metatarsals accessible to intravital microscopy in each chamber, respectively. We used only 4 mice in the case of M18 because 1 mouse was excluded due to infection of the chamber.

Intravital microscopy

For intravital microscopy, unanesthetized mice were placed in a polycarbonate tube and mounted on the stage of the microscope. During the first 4 days after implantation, measurements were performed twice a day, thereafter every day for 12 days. Images were obtained by brightfield trans-illumination microscopy using ×1.25, ×2.5, ×5, ×10 and ×20 objectives. A green filter was employed to enhance black and white contrast for better visualization of blood vessels (Leunig et al. 1994).

On days 6 and 12, a bolus of fluorescein isothiocyanate-labeled dextran (0.1 mL FITC-Dextran, Sigma Chemical Co., St. Louis, MO, at a concentration of 5 mg/100 L in 0.9% NaCl) and rhodamine 6G (0.04 mL Rh 6G, 50 mg/100 mL, Sigma Chemical Co.) were injected i.v. 5 min before microscopic examination. FITC-dextran remains within the vasculature and enables good assessment and visualization of vascular density and vascular perfusion. Rhodamine 6G stains leukocytes. FITC fluorescence was obtained by incident light using a mercury lamp, an excitation filter (485–505 nm), dichroic mirror (510 nm) and barrier filter (530 nm). Rhodamine 6G-fluorescence was obtained with an excitation filter (530–560 nm), dichroic mirror (580 nm) and barrier filter (580 nm). For analysis of mineralization, oxytetracycline (OTC 100 mg/kg b.w. in 0.9% NaCl, Pfizer, USA) was injected i.p. 6 hours later, when OTC had been cleared from non-calcified tissues, fluorescence was examined by an excitation filter (356–418 nm), a dichroic mirror (450 nm) and a

barrier filter (495 nm). All microscopic observations were recorded using a highly sensitive CCD camera, and stored on videotape for later analysis.

Angiogenesis

We described angiogenesis by determining the following parameters: (i) the appearance of vessels in the vicinity of the graft (hours), (ii) the onset of blood perfusion (hours), and (iii) the functional vascular density (FVD) of perfused and nonperfused vessels over the surface area of the graft, given in cm/cm^2. FVD was quantified by image analysis performed on a Macintosh PowerPC 7600 using the public domain NIH image program developed at the U.S. National Institutes of Health and available on the internet at http://rsb.info.nih.gov/nih-image/.

Leukocyte-endothelium interaction

We quantified the interaction of leukocytes and the inner vessel surface at day 6 and 12 after transplantation in microvessels overlying the graft. Observations were performed over a period of 30 sec in at least 3 different collecting venules with a mean diameter of 20–30 μm. Leukocytes either float freely, roll on the inner vessel surface or adhere firmly to the endothelium, i.e., stick. The quantity of floaters (FWBC) is the number of leukocytes passing a defined cross section of the vessel per unit time (10^3 cells/mm^2 s). Rollers are defined as cells travelling below 40% of the centerline velocity of the blood stream (Gaehtgens et al. 1985). The fraction of rolling cells is represented by the ratio of the number of rollers and the sum of rollers and floaters (%). The mean blood flow (10^2 mm/s) was calculated by a formula that respects the dependence of flow velocity on vessel diameter (Gaehtgens et al. 1987): $V_{mean} = V_{max} / (2–\varepsilon^2)$, where $\varepsilon = DL / DV$ is the ratio of leukocyte diameter (DL) assumed to be 7 μm (Schmid-Schonbein et al. 1980) and inner vessel diameter (DV) in μm, and Vmax is the centerline velocity. The centerline velocity V_{max} was calculated by measuring the velocity of leukocytes representing the centerline blood stream (10^2 mm/s). Stickers are identified as cells adhering to the inner surface of the vessel and thus not moving, and are quantified by the ratio of the number of stickers and the inner surface area of the vessel: number of cells / $L \times D_V \pi$ (10 cells/mm^2). The wall shear rate was calculated using Poiseuille's Law for a Newtonian fluid, $\gamma = (V_{mean} / D_V) \times 8$ (10^4/s) (Lipowsky et al. 1978, Perry and Granger 1991).

Mineralization

We assessed mineralization, given in μm, by measuring the maximal dimension in the longitudinal axis of the OTC-labeled fraction of the metatarsals, which was invisible in the absence of OTC.

Statistics

Data are presented as the mean (SD). Statistical comparisons were non-corrected and considered to be significant at a p-value < 0.05. N reflects the number of implants observed for a specific variable and could vary between different observations. This is due to the fact that in vivo phenomena occurring during the initial phase of angiogenesis are frequently difficult to image due to local tissue impairment (bleeding, inflammatory response, edema, etc.) (Leunig and Messmer 2000). This led to experimental dropouts (missing values in the statistical sense), mainly on day 12, requiring the use of an explorative rather than a confirmative statistical assessment.

For all observations, we calculated the analysis of variance. Moreover, non-parametric tests such as the Kruskal-Wallis test and Wilcoxon signed rank test were applied. Specific tests are indicated where applied.

Results

Angiogenesis

First signs of angiogenesis, identified as the appearance of blind-ending vascular tubes occurred 32 (8) hours after transplantation in M18 and 1 day later in M16 (Table 1). Accordingly, the onset of perfusion also differed between M18 and M16. On day 6, a significantly higher vascular density was measured for M18 than for M16. Based on the significant increase in vascular density in M16 from day 6 to 12, this difference in vascular density compared to M18 was absent on day 12. In contrast, vascular density for M18 did not increase significantly between day 6 and 12 (Figure).

Table 1. Angiogenesis and vascular density

	First appearance of vessels(s)	Onset of perfusion (h)	Vascular density (cm/cm^2) Day 6	Day 12	P-value [a]
M16, mean (SD)	57 (23)	65 (25)	639 (15)	967 (232)	0.04
n	15	9	8	9	
M18, mean (SD)	32 (8)	42 (13)	916 (13)	930 (88)	
n	15	10	12	7	0.1
P-value	0.002	0.01	0.004	0.2	

[a] Wilcoxon signed rank

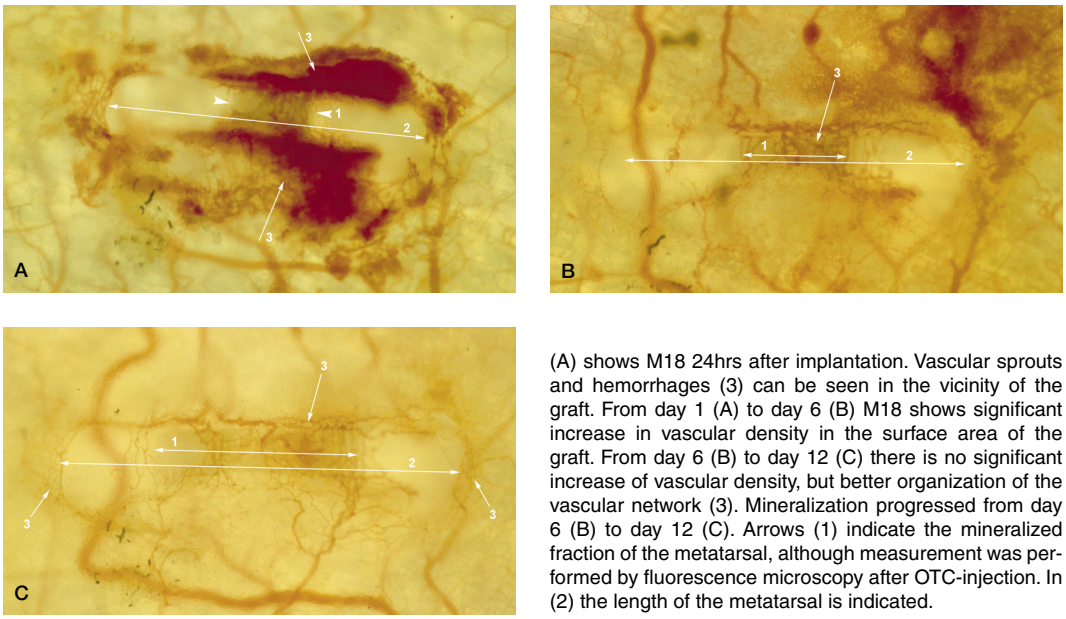

(A) shows M18 24hrs after implantation. Vascular sprouts and hemorrhages (3) can be seen in the vicinity of the graft. From day 1 (A) to day 6 (B) M18 shows significant increase in vascular density in the surface area of the graft. From day 6 (B) to day 12 (C) there is no significant increase of vascular density, but better organization of the vascular network (3). Mineralization progressed from day 6 (B) to day 12 (C). Arrows (1) indicate the mineralized fraction of the metatarsal, although measurement was performed by fluorescence microscopy after OTC-injection. In (2) the length of the metatarsal is indicated.

Table 2. Leukocyte-endothelium interaction

LEI	Floater (10^3 cells/mm^{2}s) Day 6	Day 12	Roller (%) Day 6	Day 12	Sticker (10^2 cells/cm^2) Day 6	Day 12
M16, mean (SD)	6.99 (4.97)	7.77 (4.85)	43.7 (14.7)	25.4 (13.7)	0.51 (0.82)	0.53 (0.75)
n	10	8	10	8	10	8
M18, mean (SD)	5.18 (2.30)	6.87 (4.98)	41.9 (7.0)	36.3 (12.7)	2.24 (1.65)	2.91 (2.18)
n	16	9	16	9	16	9
P-value	0.6	0.8	0.6	0.05	0.002	0.009

Leukocyte-endothelium interaction

The interaction between leukocytes and the inner vessel wall was measured in post-capillary collecting venules overlying the graft (diameter range: 20–30 μm). The quantity of floaters (FWBC) and rolling cells did not differ between M16 and M18 at days 6 and 12 (Table 2). However, a significant difference was observed for cells adhering to the vessel wall (stickers). In M18, sticker counts were elevated at both day 6 and day 12 after transplantation.

Table 3. Mineralization

	Increase from Day 0 (µm) Day 6	Day 12	P-value [a]
M16, mean (SD)	370 (200)	650 (260)	0.08
n	15	8	
M18, mean (SD)	460 (210)	650 (170)	0.02
n	14	7	
P-value	0.001	0.6	

[a] Wilcoxon signed rank

Differences in vascular shear rates could account for differences in rolling and sticking cells. Therefore, shear rate was calculated and compared between the two groups on days 6 and 12. No difference was observed (day 6, M16 n = 10, M18 n = 16, Kruskal-Wallis test, p = 0.5; day 12, M16 n = 8, M18 n = 9, Kruskal-Wallis test, p = 0.6), thereby excluding different shear rates as the cause of statistical differences in the number of rolling and sticking cells.

Mineralization

At day 6, mineralization in M18 showed a 460 (210) μm increase as compared to baseline values at day 0, whereas mineralization of M16 was reduced and measured 370 (200) μm (Table 3). Mineralization increased to the same extent in M16 and M18 until day 12. The increase in mineralization differed significantly between M16 and M18 at day 6, but not at day 12.

Discussion

Here we introduce an experimental model that allows the assessment of graft vascularization and mineralization as a function of pre-existing donor-derived microvessels. The unique aspect of this model rests on the use of fetal metatarsals known to be void of blood vessels at day 16 of gestation (M16), as evidenced by the absence of osteoclasts within the graft at this early time point (Scheven et al. 1986). Fetal long bones of specific developmental stages, representing different stages of endochondral bone formation, are well-known models for the study of chondrocyte differentiation (Dieudonne et al. 1994, Haaijman et al. 1999) or osteoclastic resorption (Van der Pluijm et al. 1991, Van Beek et al. 1993). By day 17, the perichondrium contains blood vessels, but it is not until day 18 (M18) that osteoclast-mediated bone mineralization (and thus vascularization) has started in the marrow cavity, as detected by acid phosphatase histochemistry (Scheven et al. 1986). During this process, the avascular cartilage is replaced endochondral bone formation, in which angiogenesis and osteogenesis are coupled by an endothelial cell-specific mitogen (vascular endothelial growth factor; VEGF) (Gerber et al. 1999). Since M16 and M18 differ in their developmental stage, upregulation of developmental genes is likely to have contributed to the results that were obtained.

Angiogenesis and the establishment of a vascular network is an important regulatory phenomenon for the development and repair of bone (Glowacki 1998). In M18, angiogenesis occurred significantly earlier than in M16 and vascular density was three times the vascular density of the transplantation site at day 6. Vascular density did not increase further until day 12, suggesting that sufficient vascular density was reached at day 6. In contrast, M16 showed an increase in vascular density, being significantly less than for M18 on day 6, but finally reaching the density of M18 on day 12. The high vascular density of M18 at day 6 may be due to de novo synthesis of blood vessels and/or the recruitment of pre-existing donor-derived vascular network of the graft by end-to-end anastomoses (inosculation) (Albrektsson 1980). The significantly earlier appearance of first signs of angiogenesis in M18 provides experimental evidence that pre-existing vessels of fresh osteochondral isografts may have contributed to graft vascularization by inosculation, while nonvascularized grafts need to build up their vascular system exclusively by active de novo synthesis. The ease with which effector cells can infiltrate the graft during immune surveillance is based on their ability to interact with endothelial cells lining the microvasculature. The recruitment of circulating leukocytes into the interstitial tissue is dependent on a multistep cascade of events involving sequential rolling, firm adhesion and transmigration, which are mediated by distinct adhesion and activation pathways (Springer 1994). In this study, an enhanced integrin-mediated LEI in M18 was found, revealing significantly more stickers as compared to M16. Although intravital

microscopy does not allow differentiation of pre-existing from de-novo synthesized microvessels, it is assumed that the inosculated, and therefore pre-existing and more mature vasculature of M18 is responsible for the enhanced LEI, since grafts only differed with respect to the status of their vascularization (and subsequent mineralization). This notion is supported by the finding that in microvessels induced by tissues such as tumors, LEI is diminished and almost unresponsive to biochemical stimulation (Ohkubo et al. 1991, Wu et al. 1992, Wu et al. 1994, Dellian et al. 1996). Bone mineralization, as an angiogenesis-dependent process (Winet et al. 1990), progressed in both M18 and M16 at a similar rate. This demonstrates the potential of freshly isografted metatarsals to survive and be incorporated at the recipient site.

Interpretation of our results must be done with caution, since they are based on the assumption that the multiple observations in each animal were independent. The reason for our protocol implanting 4 metatarsals in each chamber was that metatarsal bones are small in size (average length 1.5 mm) and almost transparent by the time of implantation, so that a reidentification even by microscopy was sometimes difficult. Given the small number of implants, lack of dependency cannot be proven statistically. However, the standard deviations of the implants in one chamber did not deviate extensively when compared to the overall standard deviation of the entire group for any observation, which does not suggest dependency. A statistically better approach would have been to use one metatarsal bone in one chamber each, or to implant two metatarsals, one from each group into one chamber each.

We conclude that small, developing osteochondral isografts have the potential to induce a significant angiogenic response at the implantation site. Although upregulation of developmental genes and VEGF in M18 as opposed to M16 may have contributed to the results obtained, the kinetics of revascularization and the elevated sticker counts suggest that inosculation rather than de-novo synthesis of blood microvessels caused this difference.

This work was supported by a grant from the Swiss National Science Foundation to ML. CRF was supported by the Maurice E. Müller Foundation.

No competing interests declared.

Albrektsson T. In vivo studies of bone grafts. The possibility of vascular anastomoses in healing bone. Acta Orthop Scand 1980; 51: 9-17.

Albrektsson T, Albrektsson B. Microcirculation in grafted bone. A chamber technique for vital microscopy of rabbit bone transplants. Acta Orthop Scand 1978; 49: 1-7.

Burchardt H. Biology of bone transplantation. Orthop Clin North Am 1987; 18: 187-96.

Dellian M, Witwer B P, Salehi H A, Yuan F, Jain R K. Quantitation and physiological characterization of angiogenic vessels in mice: effect of basic fibroblast growth factor, vascular endothelial growth factor/vascular permeability factor, and host microenvironment. Am J Pathol 1996; 149: 59-71.

Dieudonne S C, Semeins C M, Goei S W, et al. Opposite effects of osteogenic protein and transforming growth factor beta on chondrogenesis in cultured long bone rudiments. J Bone Miner Res 1994; 9: 771-80.

Gaehtgens P, Ley K, Pries A R, Müller R. Mutual interaction between leukocytes and microvascular blood flow. Prog Appl Microcirc 1985; 7: 15-28.

Gaehtgens P, Pries A R, Ley K. Structural, hemodynamic, and rheological characteristics of blood flow in vivo. In: Clinical hemorheology (eds. Chien S, Dormandy J, Ernst E, Matrai A). Boston: Martinus Nijhoff Publishing, 1987: 97-124.

Gerber H P, Vu T H, Ryan A M, Kowalski J, Werb Z, Ferrara N. VEGF couples hypertrophic cartilage remodeling, ossification and angiogenesis during endochondral bone formation. Nat Med 1999; 5: 623-8.

Glowacki J. Angiogenesis in fracture repair. Clin Orthop 1998: S82-9.

Haaijman A, Karperien M, Lanske B, et al. Inhibition of terminal chondrocyte differentiation by bone morphogenetic protein 7 (OP-1) in vitro depends on the periarticular region but is independent of parathyroid hormone-related peptide. Bone 1999; 25: 397-404.

Leunig M, Messmer K. Skin fold chamber models. In: Tumor angiogenesis and microcirculation (eds. Voest E E, D'amore P A). New York: Marcel Dekker, Inc., 2000: 143-54.

Leunig M, Yuan F, Berk D A, Gerweck L E, Jain R K. Angiogenesis and growth of isografted bone: quantitative in vivo assay in nude mice. Lab Invest 1994; 71: 300-7.

Leunig M, Yuan F, Berk D A, Gerweck L E, Jain R K. Heating or freezing bone. Effects on angiogenesis induction and growth potential in mice. Acta Orthop Scand 1996; 67: 383-8.

Lipowsky H H, Kovalcheck S, Zweifach B W. The distribution of blood rheological parameters in the microvasculature of cat mesentery. Circ Res 1978; 43: 738-49.

Ohkubo C, Bigos D, Jain R K. Interleukin 2 induced leukocyte adhesion to the normal and tumor microvascular endothelium in vivo and its inhibition by dextran sulfate: implications for vascular leak syndrome. Cancer Res 1991; 51: 1561-3.

Perry M A, Granger D N. Role of CD11/CD18 in shear rate-dependent leukocyte-endothelial cell interactions in cat mesenteric venules. J Clin Invest 1991; 87: 1798-804.

Puckett C L, Hurvitz J S, Metzler M H, Silver D. Bone formation by revascularized periosteal and bone grafts, compared with traditional bone grafts. Plast Reconstr Surg 1979; 64: 361-5.

Scheven B A, Kawilarang-De Haas E W, Wassenaar A M, Nijweide PJ. Differentiation kinetics of osteoclasts in the periosteum of embryonic bones in vivo and in vitro. Anat Rec 1986; 214: 418-23.

Schmid-Schonbein G W, Shih Y Y, Chien S. Morphometry of human leukocytes. Blood 1980; 56: 866-75.

Springer T A. Traffic signals for lymphocyte recirculation and leukocyte emigration: the multistep paradigm. Cell 1994; 76: 301-14.

Van Beek E, Van der Wee-Pals L, van de Ruit M, Nijweide P, Papapoulos S, Lowik C. Leukemia inhibitory factor inhibits osteoclastic resorption, growth, mineralization, and alkaline phosphatase activity in fetal mouse metacarpal bones in culture. J Bone Miner Res 1993; 8: 191-8.

Van der Pluijm G, Lowik C W, de Groot H, et al. Modulation of PTH-stimulated osteoclastic resorption by bisphosphonates in fetal mouse bone explants. J Bone Miner Res 1991; 6: 1203-10.

Winet H, Bao J Y, Moffat R. A control model for tibial cortex neovascularization in the bone chamber. J Bone Miner Res 1990; 5: 19-30

Wirtschafter Z. The genesis of the mouse skeleton. A laboratory atlas. Charles C. Thomas Springfield (Illinois) 1960: 23-7.

Wu N Z, Klitzman B, Dodge R, Dewhirst M W. Diminished leukocyte-endothelium interaction in tumor microvessels. Cancer Res 1992; 52: 4265-8.

Wu N Z, Ross B A, Gulledge C, Klitzman B, Dodge R, Dewhirst M W. Differences in leucocyte-endothelium interactions between normal and adenocarcinoma bearing tissues in response to radiation. Br J Cancer 1994; 69: 883-9.